Local Structure and the Mechanism of Response to Elastic Deformation in a Glassy Polymer

Doros N. Theodorou and Ulrich W. Suter*

Department of Chemical Engineering, Massachusetts Institute of Technology, Cambridge, Massachusetts 02139. *Received July 2, 1985*

ABSTRACT: An ensemble of undeformed and deformed model structures of a glassy amorphous vinyl polymer, atactic polypropylene, is used to probe the local structure and to explore the microscopic mechanisms of small-strain elastic deformation. The concept of atomic-level stresses is extended to bonded systems and applied to the polymer model. It is found that the chain topology influences the atomic-level stresses strongly. The structural changes brought about by shear and tension deformations are examined in detail; atomic displacements are found to deviate strongly from local affine behavior. Considerable directional correlation of atomic motion is observed both intra- and intermolecularly. Quantitative results indicate that deformation in the glassy bulk is accompanied by concerted displacement of chain segments approximately 10 bonds long. Local mechanical instability is related to the magnitude and symmetry of the changes in atomic-level stresses upon deformation.

Introduction

Recently, we introduced[1] a method for the atomistic simulation of well-relaxed amorphous polymeric glasses, and we have applied this method to glassy atactic polypropylene. Subsequently we have shown[2] that the elastic constants of polymeric glasses can be estimated theoretically by subjecting the simulated model structures to a series of deformations of small strain, and we have found[2] that the values thus obtained for atactic polypropylene glasses agree well with experimental data. We now turn to a detailed analysis of the local structure of this glass and of the molecular effect of small elastic macroscopic deformations, in an attempt to unveil the mechanism of the response to elastic deformation.

Local structure plays a central role in the properties of amorphous solids,[3] and several methods and concepts for its characterization have been introduced; among them are pair distribution functions, coordination numbers, symmetry coefficients,[4] Voronoi polyhedra,[5] and free volume.[6] In this paper local structure is characterized by *atomic-level stresses*, recently introduced by Egami, Vitek, et al.[4,7,8] for the investigation of metallic glasses; the concept is extended here to the case of systems with chemical bonds, where forces need not be "central". The local structure of an ensemble of static, undeformed, well-relaxed polypropylene model systems[1] is quantitatively examined. Also, undeformed and deformed model structures are compared, in order to detect the changes brought about by deformation; consistent trends in the microscopic mechanical response of a glassy polymer are sought.

Theory of Atomic-Level Stresses

Atomic-level stresses can serve as a basis for characterizing local structure. A brief history of this concept, which dates back to Born and Huang (1954) and has been used in the study of defects in crystalline solids, is given in ref 4. Egami, Maeda, and Vitek[4] first applied atomic-level stresses to glasses in an atomistic computer model of amorphous iron. The concept was subsequently used for studying plastic deformation in a metallic glass. Up to now, however, atomic-level stresses have been applied exclusively to nonbonded atomistic systems with central interatomic forces.

Nonbonded Systems. Essentially following ref 8, we define the atomic stress tensor for atom i, in a nonbonded system with central interatomic forces, by

$$\sigma_{i,LM} = -\frac{1}{2V_i}\sum_{j\neq i}(r_{i,L} - r_{j,L})_{\min}F^{\min}_{ij,M} \qquad (1)$$

where $\mathbf{r}_i$ and $\mathbf{r}_j$ are the position vectors of atoms i and j, $\mathbf{F}_{ij}$ is the force exerted on atom i by atom j, and V_i is a volume assigned to atom i, such that summing over all atoms gives the total volume of the system, V:

$$\sum_i V_i = V \qquad (2)$$

The indices L and M, indicating the three coordinate directions in a Cartesian system, assume the values 1, 2, and 3. The subscript or superscript "min" indicates interatomic distances and forces calculated according to the "minimum image convention".[1] Summation of all atomic-level stresses σ_i, multiplied by the appropriate volumes V_i, yields the macroscopic stress; for a system in detailed mechanical equilibrium the "internal stress tensor" σ is recovered (this is a restatement of the virial theorem[2])

$$\sigma_{LM} = (1/V)\sum_i V_i\sigma_{i,LM} \qquad (3)$$

The way in which the atomic volumes, V_i, are determined is not relevant to the physical significance of the atomic-stress tensor. A partitioning into Voronoi polyhedra could be used, but this is a laborious process, and we choose, following previous work, to assign volumes in proportion to the atomic van der Waals volumes

$$V_i = V\frac{(r_i^{\mathrm{vdW}})^3}{\sum_i (r_i^{\mathrm{vdW}})^3} \qquad (4)$$

so that all atoms belonging to the same species have the same V_i. This definition of V_i is used throughout.

Central, nonbonded interatomic forces can be written in terms of the potential energy of nonbonded interatomic interaction, $U_{ij}^{\mathrm{NB}}(r)$

$$\mathbf{F}_{ij} = \mathbf{F}_{ij}^{\mathrm{NB}} = \left.\frac{\mathrm{d}U_{ij}^{\mathrm{NB}}}{\mathrm{d}r}\right|_{r=|\mathbf{r}_i-\mathbf{r}_j|}\frac{\mathbf{r}_j - \mathbf{r}_i}{|\mathbf{r}_j - \mathbf{r}_i|} \qquad (5)$$

It follows that the atomic-level stress tensor, as defined by eq 1, is symmetric in this case (see Appendix).

The system shall be subjected to a *small homogeneous* (or affine, or quasi-continuum) deformation, characterized by a strain tensor ϵ; then, in matrix notation

$$\mathbf{r}_i^{\mathrm{affine}} = \mathbf{A}\mathbf{r}_i + \mathbf{b}, \qquad \forall i$$

$$\epsilon_i = \tfrac{1}{2}(\mathbf{A}^{\mathrm{T}}\mathbf{A} - \mathbf{I}) \simeq \tfrac{1}{2}(\mathbf{A}^{\mathrm{T}} + \mathbf{A}) - \mathbf{I} \equiv \epsilon^{\mathrm{macroscopic}} = \epsilon, \qquad |\epsilon_{LM}| \ll 1 \qquad (6)$$

The corresponding increase in total potential energy can

0024-9297/86/2219-0379$01.50/0

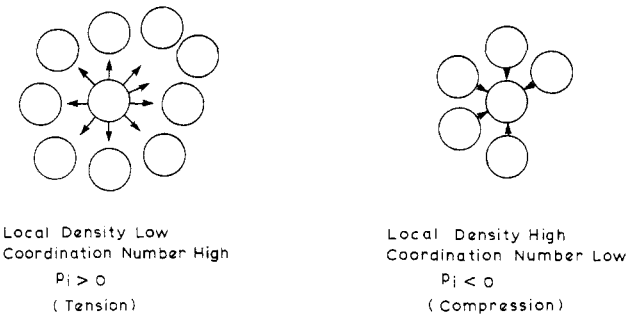

Figure 1. Physical meaning of the atomic-level hydrostatic pressure p_i in a nonbonded system.

be written as a sum of terms associated with the individual atoms[2,7]

$$\Delta U^{pot} = \sum_i \Delta U_i^{pot}$$

where, to first order in strain

$$\Delta U_i^{pot} = V_i \sum_{LM} \sigma_{i,LM} \epsilon_{LM} \tag{7}$$

terms of second and higher order in ϵ being ignored. Thus, the atomic-level stress tensor σ_i can be defined from the coefficients of the first-order term in an expansion of the potential energy associated with atom i with respect to strain for a small homogeneous deformation of the material.

Following Egami, Vitek, et al.[4,7,8] we introduce two invariants of the atomic-stress tensor for characterizing local structure. These are (a) the "atomic-level hydrostatic pressure" p_i, defined by

$$p_i = (1/3)\ \mathrm{Tr}\ (\sigma_i) \tag{8}$$

and (b) the "atomic von Mises shear stress" τ_i, defined by[9]

$$\tau_i^2 = (1/2)\ \mathrm{Tr}\ \{(\sigma_i - p_i\mathbf{I})^2\} \tag{9}$$

where $\mathbf{I}$ is the matrix representation of the unit tensor.

The sum of all p_i is the "internal pressure". Although p_i is termed a "pressure", it is really a tension or negative pressure, as is obvious from the definition in eq 8. The quantity p_i is a measure of *local density fluctuations* in the material. A high, positive value of p_i is associated with a high coordination number around atom i and with a lower than average atomic density. A low, negative value of p_i is associated with a low coordination number and with higher than average local atomic density[10] (see also Figure 1). The quantity τ_i reflects the *degree of asymmetry* of the local environment around atom i.

Systems with Rigid Bonds. We now extend the concept of atomic-level stresses to bonded systems with rigid bond lengths and bond angles. Computer models of a glassy amorphous vinyl polymer, in which molecular rearrangement can occur only through torsion around skeletal bonds,[1] provide an instance of such systems.

Forces in bonded systems are no longer central. In addition to the nonbonded interactions $\mathbf{F}_{ij}^{NB}$, given by eq 5, there are bonded forces $\mathbf{F}_{ij}^{B}$, which may have arbitrary magnitude and direction, so that

$$\mathbf{F}_{ij} = \mathbf{F}_{ij}^{NB} + \mathbf{F}_{ij}^{B} \tag{10}$$

In addition there are torques, $\boldsymbol{T}_{ij}^{B}$, exerted through the bonds[2] (a discussion of bonded forces and torques and of the methods used to obtain them is available in ref 2), and eq 1 can no longer be applied. Indeed, if one uses eq 1 with $\mathbf{F}_{ij}$ as the total (bonded + nonbonded) force, the resulting tensor σ_i is, in general, not symmetric, due to the non-central character of the bonded forces (see Appendix). Omission of the bonded contributions to $\mathbf{F}_{ij}$ (i.e., defining σ_i through eq 1, using $\mathbf{F}_{ij}^{NB}$ only in place of $\mathbf{F}_{ij}$) would lead to a symmetric σ_i but would not be meaningful, and eq 3 would no longer be satisfied.

On the basis of eq 7 we imagine the system subjected to an *infinitesimal affine* deformation, described by the strain tensor ϵ as defined in eq 6. (Note that this is possible only in the limit of infinitesimal displacements; finite-strain affine deformations are incompatible with the requirement of fixed bond lengths and bond angles.[2]) On each atom i acts as a total (bonded and nonbonded) force $\sum_{j\neq i}\mathbf{F}_{ij}$ and a total torque $\sum_{j\neq i}\boldsymbol{T}_{ij}^{B}$. Due to the infinitesimal deformation atom i will be displaced by a vector $\mathbf{dr}_i = \mathbf{r}_i^{affine} - \mathbf{r}_i^{undeformed}$ and rotated by a differential angle $(1/2)(\nabla \times \mathbf{dr})_i$ [∇ is the symbolic vector $(\mathrm{d}/\mathrm{d}x, \mathrm{d}/\mathrm{d}y, \mathrm{d}/\mathrm{d}z)$]. The total work done by the system during the deformation, equal to the work performed by all forces and all torques on all atoms, is

$$\mathrm{d}W = \sum_i (\sum_{j\neq i} \mathbf{F}_{ij})\cdot\mathbf{dr}_i + \sum_i (\sum_{j\neq i} \boldsymbol{T}_{ij}^{B})\cdot[(1/2)\nabla \times \mathbf{dr}]_i \tag{11}$$

where the first term on the right-hand side of the equation is the work of the forces (displacement of atoms) and the second term on the right-hand side is the work of the torques (rotation of bonds). Using eq 6, we obtain

$$\mathrm{d}r_{i,M} = \sum_L (A_{ML} - \delta_{ML}) r_{i,L} + b_M$$

$$(\nabla \times \mathbf{dr})_{i,K} = \sum_L \sum_M e_{LMK}(A_{ML} - \delta_{ML}) \tag{12}$$

where e_{LMK} is the alternating tensor[11] and δ_{LM} the Kronecker symbol ($\delta_{LM} = 1$ if $L = M$ and zero otherwise). Consequently

$$\mathrm{d}W = \sum_L \sum_M \{\sum_i \sum_{j\neq i} F_{ij,M} r_{i,L}\}(A_{ML} - \delta_{ML}) + \sum_M \{\sum_i \sum_{j\neq i} F_{ij,M}\} b_M + (1/2)\sum_L \sum_M \sum_K \{\sum_i \sum_{j\neq i} e_{LMK} T_{ij,K}^{B}\}(A_{ML} - \delta_{ML}) \tag{13}$$

The reciprocity of pair interactions, bonded or nonbonded,[2] yields

$$\sum_i \sum_{j\neq i} F_{ij,M} = (1/2)\{\sum_i \sum_{j\neq i} F_{ij,M} + \sum_j \sum_{i\neq j} F_{ji,M}\} = (1/2)\sum_i \sum_{j\neq i} (F_{ij,M} + F_{ji,M}) = 0 \tag{14}$$

Furthermore

$$\sum_i \sum_{j\neq i} F_{ij,M} r_{i,L} = (1/2)\{\sum_i \sum_{j\neq i} F_{ij,M} r_{i,L} + \sum_j \sum_{i\neq j} F_{ji,M} r_{j,L}\} = \sum_i \sum_{j\neq i} \{(1/2) F_{ij,M}(r_{i,L} - r_{j,L})\} \tag{15}$$

and

$$\sum_K \sum_i \sum_{j\neq i} e_{KLM} T_{ij,K}^{B} = (1/2)\sum_K \{\sum_i \sum_{j\neq i} e_{KLM} T_{ij,K}^{B} + \sum_i \sum_{i\neq j} e_{KLM} T_{ji,K}^{B}\} = \sum_K \sum_i \sum_{j\neq i} \left\{ e_{LMK} \frac{T_{ij,K}^{B} + T_{ji,K}^{B}}{2} \right\} \tag{16}$$

From these equations we obtain

$$\mathrm{d}W = \sum_L \sum_M \sum_i \left\{ \sum_{j\neq i} \frac{1}{2} \left[(r_{i,L} - r_{j,L}) F_{ij,M} + \sum_K e_{LMK} \left(\frac{T_{ij,K}^{B} + T_{ji,K}^{B}}{2} \right) \right] \right\} (A_{ML} - \delta_{ML}) \tag{17}$$

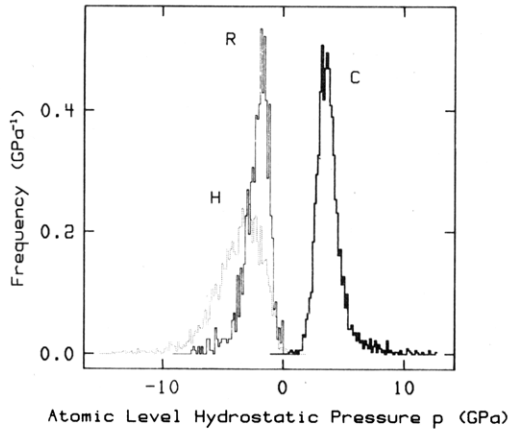

Figure 2. Distribution of the atomic-level hydrostatic pressure (p) for the three types of centers present in the model glass, atactic polypropylene (H = hydrogen, C = carbon, R = methyl). The distributions are based on 15 undeformed structures.

The term within the curly brackets is the tensor $w_{i,LM}$ and is *symmetric* (see Appendix), and

$$dW = \sum_L \sum_M \sum_i w_{i,LM}(A_{ML} - \delta_{ML}) =$$
$$\frac{1}{2}\sum_L \sum_M \{\sum_i w_{i,LM}(A_{ML} - \delta_{ML}) + \sum_i w_{i,ML}(A_{LM} - \delta_{LM})\} =$$
$$\sum_L \sum_M \sum_i w_{i,LM}\left\{\frac{1}{2}(A_{ML} + A_{LM}) - \delta_{LM}\right\} = \sum_L \sum_M \sum_i w_{i,LM}\epsilon_{LM} \quad (18)$$

The change in total potential energy associated with the imposed differential deformation is, if thermal motion is ignored

$$dU^{pot} = -dW = \sum_L \sum_M \sum_i (-w_{i,LM})\epsilon_{LM} \quad (19)$$

Comparing eq 7 and 19, we conclude that the correct definition of the atomic-level stress tensor in a bonded system is

$$\sigma_{i,LM} = -\frac{1}{V_i} w_{i,LM} =$$
$$-\frac{1}{2V_i}\sum_{j \neq i}\left\{(r_{i,L} - r_{j,L})_{\min} F^{\min}_{ij,M} + \sum_K e_{LMK}\left(\frac{T^B_{ij,K} + T^B_{ji,K}}{2}\right)\right\} \quad (20)$$

(The minimum image convention has been introduced in this expression.) For a system in detailed mechanical equilibrium the atomic-level stresses defined in eq 20 fulfill eq 3. This follows directly from the torque balances around each atom.[2] In the case of a nonbonded system, eq 20 correctly reduces to the less general form (1). With the aid of the torque balance around atom i ($\sum_{j \neq i} T^B_{ij} = 0$) eq 20 can immediately be simplified to

$$\sigma_{i,LM} = -\frac{1}{2V_i}\sum_{j \neq i}\left\{(r_{i,L} - r_{j,L})_{\min} F^{\min}_{ij,M} + \sum_K e_{LMK}\frac{T^B_{ji,K}}{2}\right\} \quad (21)$$

Distribution of Atomic-Level Stresses in a Polymer Glass

An ensemble of 15 static undeformed model structures has been described previously.[1] Atomic-level stresses were calculated here by applying eq 21 to each atom of each structure. To compensate for the use of finite-range potential energy functions,[2] a value of +98.4 MPa (from the direct integration of "potential tails"[2]) was added to the diagonal elements of σ_i. The characteristic quantities p_i and τ_i were calculated according to eq 8 and 9. The distributions of p and τ were accumulated separately for each type of center (H, C, and R = CH_3) present in our system. These distributions are plotted in Figures 2 and 3. The means and the standard deviations of the distributions are given in Table I.

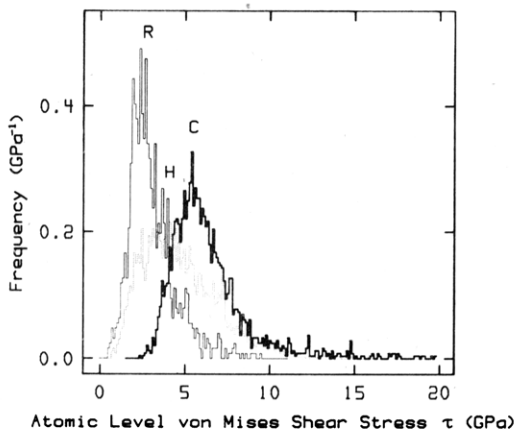

Figure 3. Distribution of the atomic von Mises shear stress (τ) for the three species present in a model glass, atactic polypropylene (see legend to Figure 2).

Table I
Characteristic Quantities of the p and τ Distributions As Depicted in Figures 2 and 3

species	$\langle p \rangle$, GPa	$\langle p^2 - \langle p \rangle^2 \rangle^{1/2}$, GPa	$\langle \tau \rangle$, GPa	$\langle \tau^2 - \langle \tau \rangle^2 \rangle^{1/2}$, GPa
hydrogen, H	−3.756	2.211	4.804	2.488
carbon, C	3.870	1.413	6.476	2.754
methyl, R	−2.209	1.214	3.091	1.459

A striking feature, evident from Figures 2 and 3, is the disparity in magnitude between the atomic-level stresses σ_i and the overall (macroscopic) internal stress σ.[2] The average diagonal element of the internal stress tensor, (1/3) Tr (σ), is equal to 82.2 MPa.[2] A typical atomic stress (Table I) is at least 30 times larger, the tails of the distributions in Figures 2 and 3 even extending to 20 GPa. In other words, there is a strong compensation effect in the summation of atomic-level stresses to the overall stress (eq 3). The large magnitude of atomic-level stresses has been pointed out by Egami, Maeda, and Vitek[4,10] for an atomic, nonbonded system (plots of those p and τ distributions are presented in ref 7). These authors observe atomic-level stresses of the same order of magnitude as those reported here.

Figure 2 reveals a distinct difference in the shape and position of the p distribution between skeletal atoms (C) on the one hand and substituents (H, R) on the other. Hydrogens and methyls are under "compression" ($p < 0$), with the p distributions skewed to the left. Carbons are under "tension" ($p > 0$), with the p distribution skewed to the right. Atomic-level stresses are obviously sensitive to the topology of bonded systems (the nonbonded, single-species results of Srolovitz, Vitek, and Egami[7] rendered a p distribution centered around zero and skewed to the left, shaped somewhat like those for H and R in Figure 2).

A detailed examination of the forces experienced by each type of center in the polypropylene model systems revealed the following: (a) Short-range nonbonded interactions (i.e., nonbonded interactions between atoms of the same chain, 3 or 4 bonds apart) are predominantly repulsive. (b) Long-range nonbonded interactions (i.e., interactions between atoms of the same chain and more than 4 bonds apart or belonging to different chains) are predominantly attractive, and weaker than short-range interactions. (c)

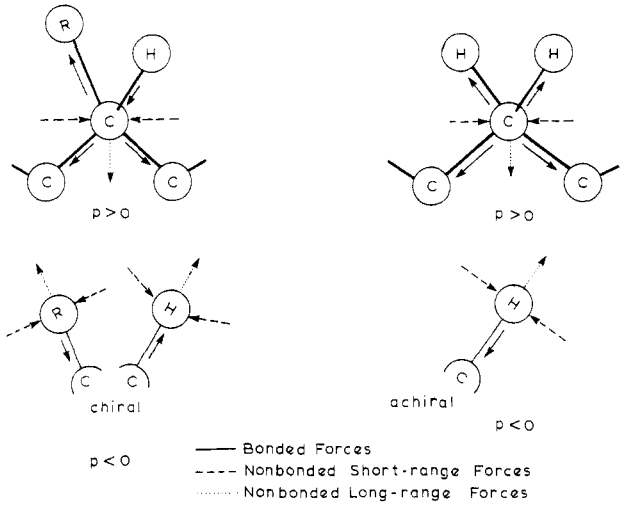

Figure 4. Stress situation in the neighborhood of each "atomic" species in the model systems. Bonded forces are pictured as central, for simplicity.

Bonded forces between skeletal carbon atoms are almost always attractive and stronger than carbon-substituent bonded forces or nonbonded forces. (d) Methine carbon/methyl substituent bonded forces are attractive, methylene carbon/pendant hydrogen bonded forces are mainly attractive, and methine carbon/pendant hydrogen bonded forces are frequently repulsive. On the basis of these observations, the stress situation created in the neighborhood of each type of center is summarized schematically in Figure 4. The compressive stress field ($p < 0$) seen in the case of substituents is mainly due to the repulsive short-range nonbonded forces. The tensile field ($p > 0$) experienced by the carbon atoms originates mainly in the strong skeletal carbon–carbon bonded forces. Let it be noted that the purely nonbonded contribution to p is compressive and follows a distribution skewed to the left for all three species considered. This confirms that carbons are differentiated from substituents in Figure 2 as a result of the special bonded forces they experience.

The spread of the p distribution reflects variations in density of the local environments. The p distribution for hydrogens is considerably wider than that of carbons and methyls (Table I). This probably originates in the fact that hydrogens come topologically in two classes, those connected to methine and those bound to methylene carbon atoms (compare Figure 4). No trace of bimodality can be discerned in the distribution, however.

The atomic shear-stress distributions (Figure 3) are all skewed to the right (this is the shape observed by Srolovitz, Vitek, and Egami[7]). The means and the standard deviations listed in Table I indicate that skeletal carbons experience the greatest asymmetry of local environments. Figure 5 contains a correlation of the p and τ values experienced by carbon atoms in all model structures. Each point corresponds to a single carbon atom. A strong positive correlation is evident; large values of p are accompanied by large values of τ and vice versa. Similar correlations are also observed in the case of the other two species studied (but not shown here). We can conclude that the atomic "stress ellipsoids" experienced by all atoms belonging to a certain species are roughly similar in shape in the undeformed state.

Microscopic Changes upon Deformation

The elastic response of amorphous glassy polypropylene to small-strain mechanical deformation has been modeled[2] by subjecting eight undeformed structures to a

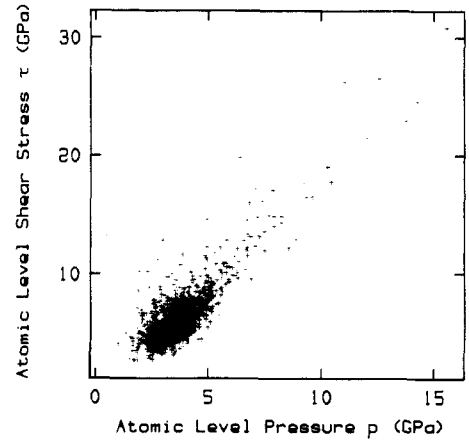

Figure 5. Correlation between atomic-level pressure and atomic-level shear stress (carbon atoms, eight undeformed structures).

"hydrostatic" compression, a "hydrostatic" tension, six shear deformations ($\pm zx$, $\pm zy$, $\pm xy$), and six uniaxial tension–compression deformations ($\pm x$, $\pm y$, $\pm z$). Here we will concentrate on the shear and uniaxial tension–compression deformations only. Thus, for each undeformed model structure 12 deformed model structures are considered, forming 6 pairs with exactly opposite macroscopic deformations. The degree of deformation,[2] ϵ, is always ± 0.001.

By direct comparison of the structural features of the deformed structures with those of the undeformed structures, from which they were obtained, we hope to be able to draw conclusions about the microscopic mechanisms of deformation.

Changes in Rotation Angles. The torsion angles of the skeletal bonds constitute the internal microscopic degrees of freedom of our model polymer chain.[1,2] The rotation angle change for bond i upon deformation is simply defined as

$$\Delta\phi_i = \phi_i^{\text{deformed}} - \phi_i^{\text{undeformed}}, \qquad 2 \le i \le 2x - 1 \qquad (22)$$

where $x = 76$ is the degree of polymerization of our "parent chains". The distribution of $\Delta\phi$ upon shear was accumulated from all shear "experiments" on all deformed model structures. A distribution of $\Delta\phi$ upon tension was similarly accumulated from all tension experiments. These distributions are displayed in Figure 6. Characteristic quantities are also given in Table II.

The $\Delta\phi$ distributions are symmetric, with average values of zero. It should be emphasized that the symmetry observed in Figure 6 is not related to the fact that pairs of opposite deformations were used for constructing them. The $\Delta\phi$ distribution for *each individual deformation is symmetric*, indicating that, at least for the small deformations studied here, torsion angles have, on the average, equal probabilities of changing in either direction (superposition of many deformations is used, here and in the following, only to reduce the statistical noise associated with a small sample size).

The standard deviation of the distribution of torsion angle changes in shear is comparable in magnitude to the macroscopic shear angle imposed on the model system during the shearing deformation (Table II). The standard deviation of the $\Delta\phi$ distribution in tension is greater than that in shear by approximately 30%. This indicates that, for the same value of ϵ, more drastic structural changes accompany tension than shear.

Atomic Displacements. Perhaps the most direct evidence of changes brought about by deformation is provided by the displacement of individual atoms. The atomic

Table II
Structural Changes upon Deformation

	shear	tension
average rotation angle change, $\langle\Delta\phi\rangle$, 10^{-3} deg	−0.12	−0.03
stand. dev of distribution of rotation angle changes, $[\langle(\Delta\phi)^2\rangle - \langle\Delta\phi\rangle^2]^{1/2}$, 10^{-3} deg	70.6	90.3
macroscopically imposed shear angle, $\tan^{-1}\epsilon$, 10^{-3} deg	57.3	–

	atomic species					
	shear			tension		
	H	C	R	H	C	R
average inhomogeneous displacement length, $\langle\|\Delta\mathbf{r}\|\rangle$, 10^{-3} Å	4.73	4.41	5.27	6.85	6.37	7.80
stand. dev of distribution of inhomogeneous displacement lengths, $[\langle\|\Delta\mathbf{r}\|^2\rangle - \langle\|\Delta\mathbf{r}\|\rangle^2]^{1/2}$, 10^{-3} Å	6.05	5.75	7.09	5.73	5.33	6.80
average affine displacement length corresponding to the same deformation, $\langle\|\Delta\mathbf{r}^{\text{affine}}\|\rangle$, 10^{-3} Å	4.54	4.54	4.54	4.54	4.54	4.54
relative atomic displacement length in the limit of large distances, $\lim_{\|\mathbf{r}_i-\mathbf{r}_j\|\to\infty}\|\Delta\mathbf{r}_i - \Delta\mathbf{r}_j\|$, 10^{-3} Å	7.09	6.67	7.89	9.93	9.31	11.14
$[\lim_{\|\mathbf{r}_i-\mathbf{r}_j\|\to\infty}\|\Delta\mathbf{r}_i - \Delta\mathbf{r}_j\|]/\langle\|\Delta\mathbf{r}\|\rangle$	1.49	1.51	1.49	1.45	1.46	1.43

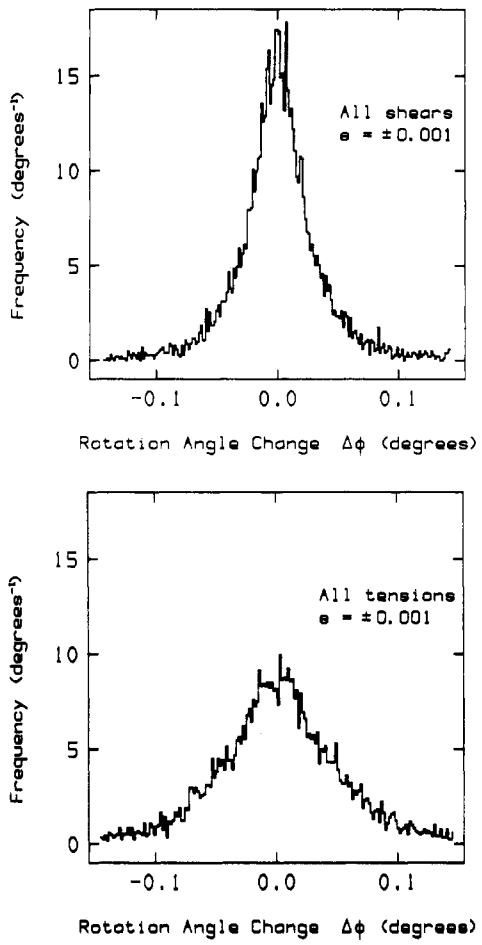

Figure 6. (a) Distribution of rotation angle changes upon shear (eight structures, six shear experiments per structure). (b) Distribution of rotation angle changes upon tension (eight structures, six tension experiments per structure).

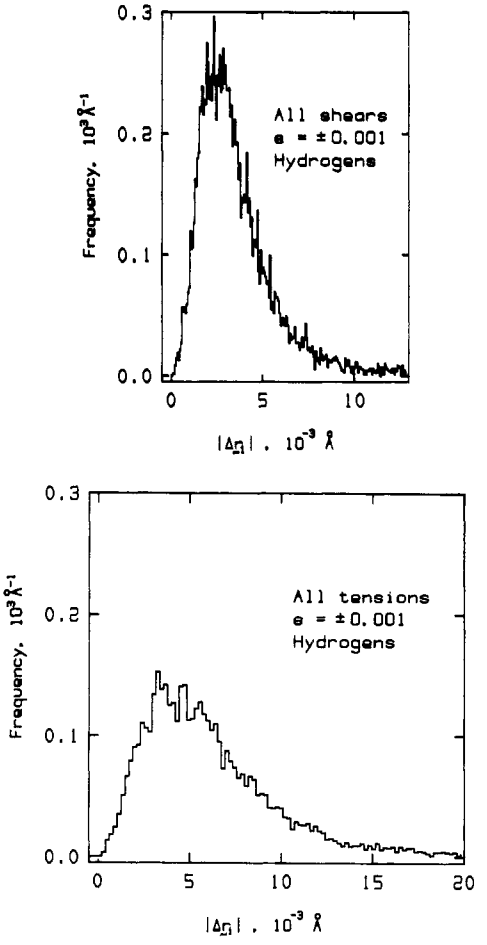

Figure 7. (a) Distribution of inhomogeneous displacement lengths of hydrogen atoms upon shear (eight structures, six shear experiments per structure). (b) Distribution of inhomogeneous displacement lengths of hydrogen atoms upon tension (eight structures, six shear experiments per structure).

displacements reflect not only local topological changes in the material but also the macroscopic (externally imposed) strain field. For example, the total displacements of atoms in the vicinity of two opposite faces of the "periodic box" would appear correlated during shear simply because of the parallelity of the faces. To study strictly local, microscopic, rearrangements, we *subtract the affine contribution from all displacements.*

We define the "*inhomogeneous displacement vector*" of atom i as the difference

$$\Delta\mathbf{r}_i = \mathbf{r}_i^{\text{deformed}} - \mathbf{r}_i^{\text{affine}} \tag{23}$$

where $\mathbf{r}_i^{\text{deformed}}$ is the position vector of the atom in the deformed system and $\mathbf{r}_i^{\text{affine}}$ is the position that this atom would have if we subjected the undeformed system to a (hypothetical) strictly affine deformation, characterized by the same macroscopic strain tensor as the actual deformation, and such that the centers of mass of the (hypothetical) affinely deformed and of the actual deformed system coincide.

As discussed earlier,[2] strictly affine deformations in the systems treated here are impossible because of the constraints imposed by fixed bond lengths and bond angles. The magnitude of $\Delta\mathbf{r}_i$ is a direct measure of the deviation from affine behavior, sensitive to local rearrangements in the vicinity of atom i. The distributions of this "inhomogeneous displacement length" were accumulated for each type of center from all shear and all tension deformations. The distributions for hydrogens are presented in Figure 7. The distributions for carbon atoms and methyl groups (not shown here) are very similar. The

characteristic quantities of all distributions are summarized in Table II. All $|\Delta \mathbf{r}|$ distributions are skewed to the right. Displacements tend to be largest for methyl groups, hydrogens follow, and carbon atoms experience the smallest displacements. This can be understood if we view the motion of substituents as the superposition of a rotation about the chain backbone and of the displacement of skeletal carbons; C–R bonds are longer than C–H bonds, so that methyl groups move about a longer "arm", and $\langle|\Delta \mathbf{r}|\rangle$ should be larger than for hydrogens. Within a given species, the average inhomogeneous displacement in tension is larger than that in shear by approximately 45%. This again suggests more drastic topological changes.

The average *affine* displacement length corresponding to the studied deformations can be obtained by continuum geometry. For a cube of edge length a, sheared to a strain ϵ so that its center remains unchanged,

$$\langle|\Delta \mathbf{r}^{\text{affine}}|\rangle = \epsilon a/4 \qquad \text{(shear)} \tag{24}$$

For the same cube, extended uniaxially to a strain ϵ in a transformation that leaves its center unchanged

$$\langle|\Delta \mathbf{r}^{\text{affine}}|\rangle = \epsilon a/4 \qquad \text{(tension)} \tag{25}$$

Using[2] $a = 18.15$ Å and the extent of deformation $\epsilon = 0.001$, we arrive at a value of $\langle|\Delta \mathbf{r}^{\text{affine}}|\rangle = 4.54 \times 10^{-3}$ Å. Comparing with the $\langle|\Delta \mathbf{r}|\rangle$ values listed in Table II, we conclude that the average inhomogeneous displacement length is comparable to the average affine displacement length corresponding to the same deformation. In other words, on an atomistic scale there is a strong nonaffine component to the deformation of a polymeric glass.

In order to investigate the motion of atoms relative to each other, we define the *relative inhomogeneous displacement vector* for a pair of atoms i and j as the difference $(\Delta \mathbf{r}_i - \Delta \mathbf{r}_j)$. We would expect the length of this vector to be a function of interatomic separation. Neighboring atoms would tend to move together and so would give a low value of $|\Delta \mathbf{r}_i - \Delta r_j|$ (which is called the *relative inhomogeneous displacement length*). The relative inhomogeneous displacement length should increase continually with interatomic distance, approaching a limit corresponding to completely uncorrelated motion of the atoms considered. Indeed, such a behavior is observed. In Figure 8 we present $|\Delta \mathbf{r}_i - \Delta \mathbf{r}_j|$ as a function of $|\mathbf{r}_i - \mathbf{r}_j|$ for hydrogen atoms in all shears and tensions performed. (The minimum image convention is always used in determining interatomic separations.) The corresponding plots for carbons and methyls (not shown here) are very similar. The asymptotic values reached in the limit of high interatomic separations are listed in Table II and can be compared with the average inhomogeneous displacement length $\langle|\Delta \mathbf{r}|\rangle$. If the vectors $\Delta \mathbf{r}_i$ and $\Delta \mathbf{r}_j$ consisted of completely uncorrelated components, distributed according to a Gaussian law, then the ratio $\langle|\Delta \mathbf{r}_i - \Delta \mathbf{r}_j|\rangle / \langle|\Delta \mathbf{r}|\rangle$ would assume a value of $2^{1/2}$. From Table II we see that this ratio is observed, within the limits of statistical noise, for high interatomic separations. The displacements of atoms lying as close as ca. 10 Å are completely independent.

Directional Correlation of Displacements. To quantitatively characterize directional correlation we consider the angle $\theta = \cos^{-1}(\Delta \mathbf{r}_i \cdot \Delta \mathbf{r}_j / |\Delta \mathbf{r}_i||\Delta \mathbf{r}_j|)$ between the inhomogeneous displacement vectors of each pair of atoms and form the function

$$S(r) = (1/2)\{3\langle\cos^2\theta(r)\rangle - 1\} \tag{26}$$

where the average is taken over all atom pairs at a distance $|\mathbf{r}_i - \mathbf{r}_j| = r$ from each other. Plots of $S(r)$ for hydrogens are presented in Figure 9. One sees strong directional correlations (i.e., tendencies for parallelity) between

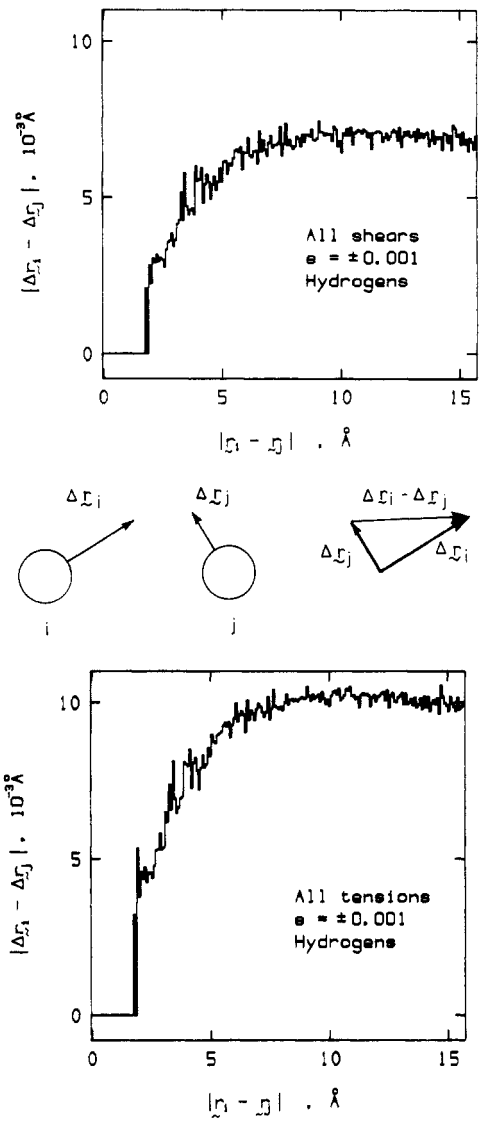

Figure 8. (a) Relative inhomogeneous displacement length as a function of interatomic distance, for hydrogen atoms in all shear deformations studied (eight structures, six shear experiments per structure). (b) Relative inhomogeneous displacement length as a function of interatomic distance, for hydrogen atoms in all tension deformations studied (eight structures, six tension experiments per structure).

neighboring atoms; this trend decreases "quasi-exponentially" with increasing distance. Again, there is no correlation at large distances. We also accumulated the purely *intermolecular* directional correlation function from atom pairs belonging to *different images of the parent chain* only. The intermolecular $S(r)$ is a measure of how deformation "hops"[12] from chain to chain in the bulk. It, too, displays some correlation at short distances (Figure 9), which, however, is considerably weaker than the total.

The directional correlation of the inhomogeneous displacements of atoms belonging to the *same* chain is examined in Figure 10 (again, only plots for hydrogen atoms are shown, but the behavior for the other two atomic species is very similar). The angle θ between displacement vectors is considered and the quantity

$$S_k = (1/2)\{3\langle\cos^2\theta_k\rangle - 1\} \tag{27}$$

formed, where the average is taken over all atom pairs attached to segments (k_1, k_2) belonging to the same chain and separated by a fixed number of bonds $k = k_1 - k_2$. This intramolecular S_k is plotted against the number of intervening bonds, k. We see strong directional correlation

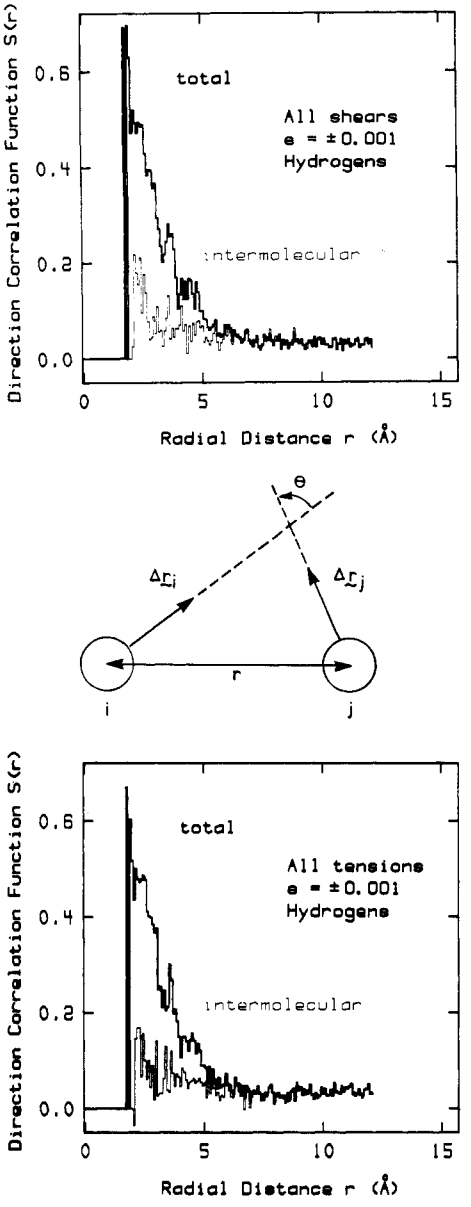

Figure 9. Directional correlation of inhomogeneous displacements as a function of interatomic distance in the bulk, for hydrogen atoms: (a) all shear deformations studied (eight structures, six shear experiments per structure); (b) all tension deformations studied (eight structures, six tension experiments per structure).

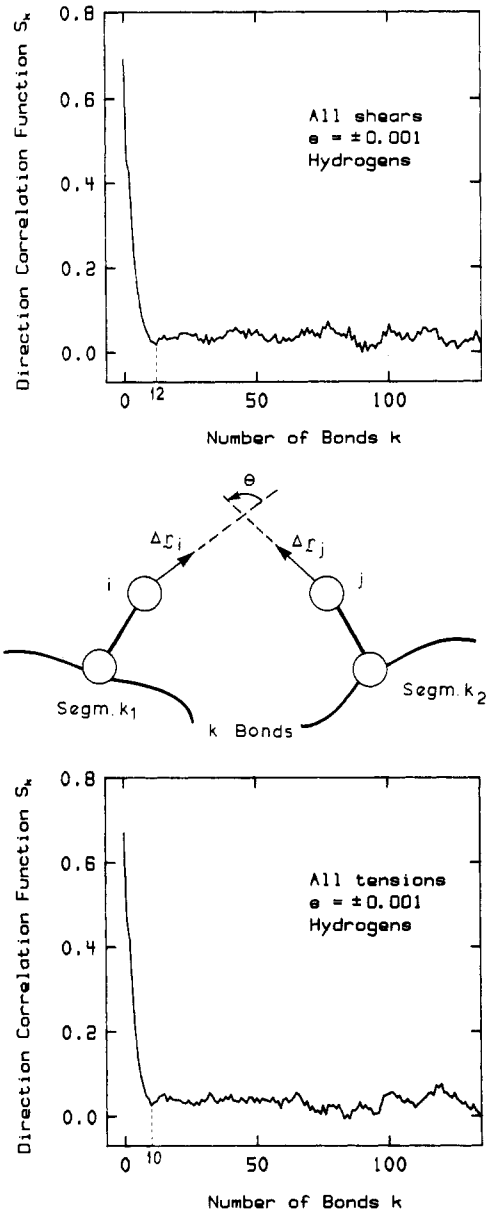

Figure 10. Directional correlation of inhomogeneous displacements of hydrogen atoms belonging to the same parent chain as a function of the number of skeletal bonds (k) between the segments to which the atoms are attached: (a) all shear deformations studied (eight chains, six shear experiments per structure); (b) all tension deformations studied (eight chains, six tension experiments per structure).

at small separations, which however drops quickly to a value of practically 0; 12 bonds in the case of shear and 10 in the case of tension suffice. Thus, our model results indicate that deformation in the glass is accompanied by coordinated displacement of chain segments approximately 10 bonds long.

Changes in Atomic-Level Stresses upon Deformation. Atomic-level stresses reflect the characteristics of the local environment around each atom. Hence, the changes

$$\Delta p_i = p_i^{\text{deformed}} - p_i^{\text{undeformed}}$$
$$\Delta \tau_i = \tau_i^{\text{deformed}} - \tau_i^{\text{undeformed}} \quad (28)$$

are direct quantitative measures of local structural changes brought about by deformation.

In Figure 11 Δp is plotted against $\Delta \tau$ for all carbon atoms of a typical model structure subjected to shear deformations. We observe a pronounced positive correlation between Δp and $\Delta \tau$ and conclude that large changes in local density upon elastic deformation generally occur under retention of the shape of the atomic stress ellipsoids (compare Figure 5).

A remarkable feature of the pattern displayed in Figure 11 is its almost perfect central symmetry. The points in this pattern have been obtained from three pairs of opposite ($\epsilon = \pm 0.001$) shearing deformations ($\pm zx$, $\pm zy$, $\pm xy$). The symmetry observed indicates that, within the range of deformations considered, for a "normal" structure (see below), opposite macroscopic deformations induce exactly opposite microscopic changes in local atomic environment. Indeed, it has been confirmed that the displacement vectors of all atoms are strictly antiparallel, and of very similar magnitude, for such pairs of deformations, although deviations from affine behavior are strong.

It has been mentioned[2] that two of the eight model structures investigated exhibit thermodynamic instability (the matrix of isothermal elastic coefficients is not positive definite) when subjected to deformation. One of these

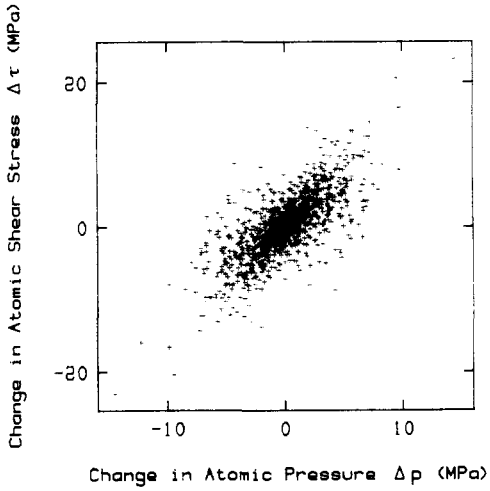

Figure 11. Changes in the atomic-level hydrostatic pressure p, plotted against changes in the atomic-level shear stress τ, for carbon atoms in a typical model structure subjected to shear. The plotted points are from six shear deformations on a single structure.

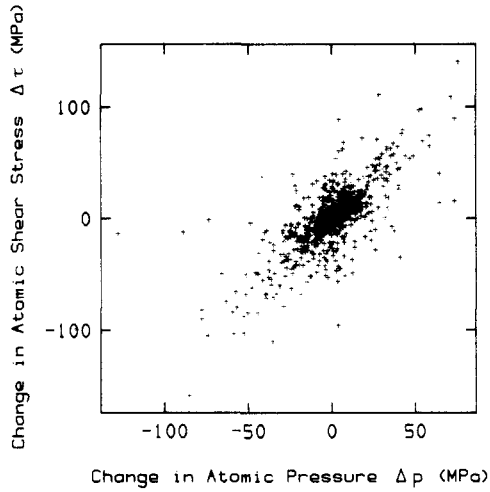

Figure 12. Changes in the atomic-level hydrostatic pressure p, plotted against changes in the atomic-level shear stress τ, for carbon atoms in a model structure exhibiting thermodynamic instability when subjected to shear. The plotted points come from six shear deformations on a single structure.

structures is strongly "abnormal", in that it gives negative shear moduli in two of the three modes of shearing examined. In Figure 12 we plot Δp vs. $\Delta\tau$ for this structure; this graph is completely analogous to Figure 11. Two observations can be made immediately: (a) The magnitude of atomic-level stress changes in this unstable structure is at least 5 times that in a "normal" structure. (b) The pattern is no longer symmetric, especially near its fringes. The excessive topological rearrangement and the lack of microscopic symmetry, laid bare by Figure 12, is observed only in this single unstable structure. Furthermore, it stems solely from the two "abnormal" modes of shearing deformation. The contribution of the third shear mode, which is mainly responsible for the cluster of points at the center of the pattern, is symmetric and of ordinary magnitude, resembling Figure 11. Closer examination has revealed that a particular portion of the parent chain undergoes vigorous motion (relative to the small strains) when an "abnormal" shear is imposed, with displacements that change in magnitude by more than a factor of 2 when the direction of shear is reversed.

In their study of plastic deformation in an amorphous metal Srolovitz, Vitek, and Egami[7] observed well-defined localized deformation events. Collective, two-dimensional sliding motions of groups involving approximately 8 atoms as well as circular, three-dimensional motions of groups of approximately 14 atoms were seen, and large τ values ("τ defects") were found to be associated with deformation sites. The present study, carried out with a range of strains much smaller than theirs (within the elastic regime), did not reveal *any* significant correlation between τ (or p) and atomic displacements. Such correlations might, however, appear at larger strains, where plastic deformation becomes important.

Acknowledgment. We gratefully acknowledge support from the National Science Foundation (Polymers Program) under Grant No. DMR-8312694 and the Texaco-Mangelsdorf Associate Professorship at the Massachusetts Institute of Technology. We also thank Professors T. Egami and V. Vitek for invigorating discussions.

Appendix. Symmetry of the Atomic-Level Stress Tensor

Systems with Exclusively Central Forces. In the case of a nonbonded system with central forces, the condition of symmetry of the tensor σ_i, defined by eq 1, becomes $\sigma_{i,LM} = \sigma_{i,ML}$; hence

$$\sum_{j\neq i}[(r_{i,L} - r_{j,L})_{\min}F^{\min}_{ij,M} - (r_{i,M} - r_{j,M})_{\min}F^{\min}_{ij,L}] = 0 \qquad \forall(L,M)\in\{1, 2, 3\}^2$$

This is equivalent to the statement

$$\sum_{j\neq i}(\mathbf{r}_j - \mathbf{r}_i)_{\min} \times F^{\min}_{ij} = \mathbf{0} \tag{A.1}$$

Since the central force $\mathbf{F}^{\min}_{ij}$ is collinear with the vector $(\mathbf{r}_j - \mathbf{r}_i)_{\min}$ (eq 5), eq A.1 is fulfilled, and tensor σ_i is symmetric.

Bonded Systems. In the presence of noncentral bonded forces eq A.1 is no longer true, and the tensor defined by eq 1 is no longer symmetric. We defined the atomic-level stress tensor by eq 20. The tensor σ_i is symmetric if, and only if, the tensor $\mathbf{w}_i$ (see eq 17 and 18) is symmetric. Here we prove the symmetry of this tensor. Symmetry of $\mathbf{w}_i$, i.e., $w_{i,LM} = w_{i,ML}$, is tantamount to

$$\sum_{j\neq i}\left\{(r_{i,L} - r_{j,L})_{\min}F^{\min}_{ij,M} - (r_{i,M} - r_{j,M})_{\min}F^{\min}_{ij,L} + \sum_K e_{LMK}\frac{T^{B}_{ij,K} + T^{B}_{ji,K}}{2} - \sum_K e_{MLK}\frac{T^{B}_{ij,K} + T^{B}_{ji,K}}{2}\right\} = 0$$

Since $e_{LMK} = -e_{MLK}$

$$\sum_{j\neq i}\{(r_{i,L} - r_{j,L})_{\min}F^{\min}_{ij,M} - (r_{i,M} - r_{j,M})_{\min}F^{\min}_{ij,L} + \sum_K e_{LMK}(T^{B}_{ij,K} + T^{B}_{ji,K})\} = 0$$

and

$$\sum_K\sum_{j\neq i}\{[(\mathbf{r}_i - \mathbf{r}_j)_{\min} \times F^{\min}_{ij}]_K e_{LMK} + (\boldsymbol{T}_{ij}{}^{B} + \boldsymbol{T}_{ji}{}^{B})_K e_{LMK}\} = 0$$

For this equation to hold $\forall(L, M) \in \{1, 2, 3\}^2$ it is necessary and sufficient that

$$\sum_{j\neq i}[(\mathbf{r}_i - \mathbf{r}_j)_{\min} \times \mathbf{F}^{\min}_{ij} + \boldsymbol{T}_{ij}{}^{B} + \boldsymbol{T}_{ji}{}^{B}] = \mathbf{0}$$

Decomposing the force $\mathbf{F}_{ij}$ into its bonded and nonbonded part, as in eq 10, and realizing that the nonbonded part is collinear with the interatomic vector (eq 5), we obtain equivalently

$$\sum_{j \neq i} [(\mathbf{r}_i - \mathbf{r}_j)_{\min} \times \mathbf{F}_{ij}^{B} + \boldsymbol{T}_{ij}^{B} + \boldsymbol{T}_{ji}^{B}] = \mathbf{0} \quad \text{(A.2)}$$

If centers i and j are not connected by a bond, all terms in the bracket of eq A.2 automatically vanish. In case atoms i and j are bonded to each other, the torque balance on bond ij (Appendix B of ref 2) gives

$$(\mathbf{r}_i - \mathbf{r}_j) \times (-\mathbf{F}_{ij}^{B}) + (-\boldsymbol{T}_{ij}^{B}) + (-\boldsymbol{T}_{ji}^{B}) = \mathbf{0}$$

or

$$(\mathbf{r}_i - \mathbf{r}_j)_{\min} \times \mathbf{F}_{ij}^{B} + \boldsymbol{T}_{ij}^{B} + \boldsymbol{T}_{ji}^{B} = \mathbf{0}$$

and the contribution from bonded pair ij is again zero. Thus eq A.2 is true, which proves the symmetry of tensors $\mathbf{w}_i$ and σ_i.

Registry No. Polypropylene (homopolymer), 9003-07-0.

References and Notes

(1) Theodorou, D. N.; Suter, U. W. *Macromolecules* **1985**, *18*, 1467–1478.
(2) Theodorou, D. N.; Suter, U. W. *Macromolecules*, in print.
(3) Zallen, R. "The Physics of Amorphous Solids"; Wiley: New York, 1983; Chapter 2.
(4) Egami, T.; Maeda, K.; Vitek, V. *Philos. Mag.* **1980**, *41*, 883–901.
(5) Maeda, K.; Takeuchi, S. *Philos. Mag. A* **1981**, *44*, 643–656. Weber, T. A.; Stillinger, F. H. *J. Chem. Phys.* **1981**, *74*, 4020–4028.
(6) Cohen, M. H.; Grest, G. S. *Phys. Rev. B* **1979**, *20*, 1077–1098. Grest, G. S.; Cohen, M. H. *Adv. Chem. Phys.* **1981**, *48*, 455–525.
(7) Srolovitz, D.; Vitek, V.; Egami, T. *Acta Metall.* **1983**, *31*, 335–352.
(8) Egami, T.; Vitek, V. *J. Non-Cryst. Solids* **1984**, *61–62*, 499–510.
(9) Timoshenko, S. P.; Goodier, J. N. "Theory of Elasticity"; 3rd Ed.; McGraw-Hill: New York, 1970; p 224.
(10) Egami, T.; Vitek, V. "Local Structural Fluctuations and Properties of Amorphous Metals"; Proceedings of Symposium on Amorphous Materials: Modeling of Structure and Properties, AIME, Oct 25 and 26, 1982.
(11) Jeffreys, H. "Cartesian Tensors"; Cambridge University Press: Cambridge, UK, 1969.
(12) Yannas, I. V. *Proc. Int. Symp. Macromol.* **1975**, 265–285. Yannas, I. V.; Luise, R. R. In "The Strength and Stiffness of Polymers"; Zachariades, A. E., Porter, R. S., Ed.; Marcel Dekker: New York, 1983.

Dynamical Properties of High Molecular Weight Polystyrene in the Dilute–Semidilute Transition Region in Cyclopentane at the Θ Temperature

Wyn Brown

Institute of Physical Chemistry, University of Uppsala, 751 21 Uppsala, Sweden.

Received January 2, 1985

ABSTRACT: Data for the polystyrene ($M = 8 \times 10^6$ and $M = 15 \times 10^6$)/cyclopentane Θ system (Θ = 21 °C) are presented. Quasi-elastic light scattering measurements were made on semidilute solutions in the high-q region to characterize the gel mode. The time correlation function was found to be consistent with a bimodal expression including a small base-line term, as predicted by Brochard: exponent 1, a gel mode of low-intensity amplitude and concentration independent over the interval up to about $10C^*$; exponent 2, a slower hydrodynamic mode of the same magnitude as that evaluated with the cumulants method at low q values. This mode is of dominant amplitude and has a small negative dependence on concentration. Both relaxations were found to be q^2-dependent and also independent of molecular weight. The presence of two cooperative modes illustrates the fundamentally heterogeneous character of Θ semidilute solutions. The results are in agreement with the predictions of Brochard for the gel mode. The hydrodynamic mode, however, does not exhibit the anticipated linear dependence on concentration in the interval studied. The present data also indicate the presence of a very slow relaxation that has been assigned to a base-line term in the bimodal analysis of the faster decays. Its amplitude increases with concentration and also more weakly with decreasing angle at a given concentration. The estimated relaxation rate when approximated as a third exponential changes with the sampling time used.

Introduction

Brochard and de Gennes[1] and Brochard[2] treated the dynamics of semidilute polymer solutions in Θ solvents. Their model assumes two elastic moduli (the osmotic and gel moduli), and thus two modes are potentially observable in dynamic light scattering experiments. Entanglements will lead to a transient network[3] of lifetime T_R. If $\Gamma T_R < 1$ (where Γ is the relaxation rate associated with the concentration fluctuations), then the chains are able to disentangle during a diffusion time $(D_s q^2)^{-1}$. Here q^2 is the scattering vector and D_s is a "slow" cooperative diffusion coefficient (an osmotic diffusion coefficient, related to the osmotic modulus), which is predicted to be directly proportional to concentration. By observations at sufficiently small q, in the hydrodynamic limit, one should be able to determine D_s. On the other hand, at high frequencies when $\Gamma T_R > 1$, a fast gel-like mode (D_g) should be detectable above the threshold value of q defined by the relationship

$$q_g^2 = (T_R D_g)^{-1} \quad (1)$$

D_g is predicted to be independent of concentration. The model of Brochard[2] thus leads to a bimodal character for the dynamic structure factor, $S(q,t)$, in the gel region with the participation of D_s and D_g. However, a very slow q-independent relaxation is also suggested as existing together with D_g and D_s.

Solely from an experimental viewpoint, there is abundant evidence that the semidilute solution structure in Θ media is more complicated than that in good solvents. Few studies exist of such systems using quasi-elastic light scattering (QELS). This is partly a consequence of the relatively high monomer concentrations required to attain C^* in Θ solvents and also the emphasized problems of working with highly self-entangled polymers and particu-

0024-9297/86/2219-0387$01.50/0